A Fiber-Optic Ultrasonic Visualization Technique for Damage Detection in a 1000 °C Environment

Fengming Yu, Osamu Saito, Yoji Okabe, and Zixuan Li

Abstract Heat-resistant structures constitute important civil infrastructure, such as thermal and nuclear power plants. Structural health monitoring (SHM) techniques based on the measurement of ultrasonic guided waves are expected to evaluate the reliability of the aging heat-resistant structures at high temperatures. However, since commercial piezoelectric acousto-ultrasonic actuators and sensors have a limited heat resistance up to 200 °C, they are inapplicable to establishing the high-temperature SHM. Optical fiber acoustic sensors (OFAS) are potential candidates for high-temperature acoustic sensing because they are made from silica glass that withstands temperatures exceeding 1000 °C. As one type of OFAS, fiber-optic Bragg grating (FBG) sensing systems have been developed to detect ultrasonic waves with a high sensitivity comparable to the PZT sensors. The purpose of this research is to build a high-temperature in-situ damage diagnosis using a laser ultrasonic visualization system combined with a remote FBG-based sensing configuration. In this method, an ultrasonic wave is excited by the laser irradiation on the surface of a material and then received by the remotely installed FBG sensor. Because both wave excitation and wave sensing parts have excellent heat resistance, the proposed system enables a stable ultrasonic measurement at elevated temperatures. In this article, the ultrasonic visualization was demonstrated in a specimen of heat-resistant material at a temperature of 1000 °C. A wavenumber-frequency analysis based on a three-dimensional Fourier transform was also conducted to extract the wave components corresponding to the reflection caused by an artificial defect in the specimen. As a result, the filtered visualization results enabled precise damage detection in the high-temperature environment.

Keywords Structural health monitoring · High-temperature environment · Optical fiber ultrasonic sensor · Ultrasonic visualization · Laser ultrasonics · Damage diagnostics

F. Yu (✉) · O. Saito · Y. Okabe
Institute of Industrial Science, The University of Tokyo, Tokyo, Japan
e-mail: houmei@iis.u-tokyo.ac.jp

Z. Li
School of Engineering, The University of Tokyo, Tokyo, Japan

Z. Wu et al. (eds.), *Experimental Vibration Analysis for Civil Engineering Structures*,
Lecture Notes in Civil Engineering 224,
https://doi.org/10.1007/978-3-030-93236-7_15

1 Introduction

High-temperature structural health monitoring (SHM) techniques are expected to ensure the reliability of aging heat-resistant structures constituting thermal and nuclear power plants. As an SHM method, the inspection with guided ultrasonic waves is sensitive to microscopic damages over a large area. Hence, the method can effectively evaluate the global integrity of large-scale structures by monitoring the damage occurrence [1]. Piezoelectric acousto-ultrasonic actuators and sensors are widely used to establish the SHM methods at room temperatures [2]. However, it is difficult to apply those devices at high temperatures due to their limited heat resistance up to 200 °C.

In contrast, optical fiber sensors are attractive for establishing high-temperature sensing technologies because they are inscribed in silica-glass fibers with good resistance to high temperatures exceeding 1000 °C [3]. As a type of optical fiber sensor, fiber-optic Bragg grating (FBG) sensors have been widely used for ultrasonic measurement [4]. The FBG is a periodic perturbation of the refractive index along the core of a single-mode optical fiber [5]. When an input light propagates through the FBG in the optical fiber, reflections occur along the grating due to the refractive index's variation. The reflected wavelength is known as the Bragg wavelength. A dynamic strain in the FBG mainly leads to the change in the grating pitch, thus shifting the Bragg wavelength of FBGs. Hence, the ultrasonic strain wave can be detected by demodulating the wavelength shift with high-speed interrogation systems.

However, compared with PZT sensors, the conversational FBG sensors have a relatively low ultrasonic sensitivity. To enhance the sensitivity, a phase-shifted FBG (PSFBG) has been widely introduced in the development of fiber-optic ultrasonic sensing systems [6]. The PSFBG is manufactured by inserting a phase shift into the periodic perturbation of the refractive index. The inserted phase shift point induces an additional narrow dip with a steep linear slope in the middle of the reflectivity spectrum. Taking advantage of the spectral characteristic, Wu and Okabe [7] developed a PSFBG balanced ultrasonic sensing system with a high sensitivity comparable to the PZT sensors. Another major advantage of the PSFBG is the short effective gauge length concentrated around the phase-shifted point. This characteristic enables a response to the ultrasonic wave with an extremely short wavelength, thus broadening the sensing frequency bandwidth.

Unfortunately, the FBG-type sensing systems are unapplicable at high temperatures because the optical gratings inscribed in the core of optical fibers become unstable at temperatures exceeding 400 °C and vanish at 900 °C. To overcome the problem, the authors constructed a PSFBG-based remote ultrasonic sensing configuration [8]. In the configuration, a point of the optical fiber is bonded on the structure at high temperature, and the PSFBG is placed away from the high-temperature environment. Then the optical fiber is used as an ultrasonic waveguide to transmit ultrasonic waves from the bonding point on the structure to the PSFBG in the room temperature environment. Since the ultrasonic waveguide formed by the optical fiber has great

heat resistance, this remote adhesion configuration can receive ultrasonic waves at a temperature of up to 1000 °C with high sensitivity and excellent stability.

With the help of the remote sensing configuration, we established a passive method with the PSFBG sensor by the measurement of damage-induced acoustic emission (AE) signals in heat-resistant materials at a temperature as high as 1000 °C [9]. The AE measurement is effective in real-time damage monitoring but is unable to detect existing damages. In practice, an active method is also required for the evaluation after the damages appear in the structures.

In the traditional active methods based on FBG sensing, the PZT-made actuators are widely used to excite the ultrasonic wave. However, it is difficult to use the PZT devices at high temperatures due to their low heat resistance, as previously mentioned. To resolve the problem, we combined the remote sensing method with a laser ultrasonic excitation. A non-contact manner makes the laser ultrasonic excitation attractive for the application in a harsh environment. Moreover, many papers [10–14] have expanded the use of laser ultrasonics to visualize the propagation of ultrasonic guided waves in structures. Since the inspection with ultrasonic visualization can realize reliable and intuitive damage identification, many related methods are researched and developed to diagnose aircraft structures and civil structures.

Details about the configuration of our proposed laser ultrasonic sensing system and the principle of wave visualization are described in the next chapter. Then, in Chap. 3, an experiment will demonstrate that the system effectively visualizes the propagation of ultrasonic waves in a ceramic specimen at elevated temperatures. Furthermore, a signal processing for extracting the damage-induced reflection wave from the visualization results enables precise detection of an artificial defect in the specimen at a temperature as high as 1000 °C.

2 Ultrasonic Visualization System

2.1 System Configuration

In the laser ultrasonic excitation, a pulsed laser beam is irradiated onto the surface of a material, as depicted on the left side of Fig. 1. An elastic wave is induced by the thermal expansion around the point of laser illumination [15]. This non-contact way protects the laser oscillator from thermal exposure to achieve a stable wave excitation at elevated temperatures. Also, the position of the laser illumination point can be specified by controlling the direction of the laser beam.

In this research, a system of laser ultrasonic visualizing inspector (LUVI-CP2, Tsukuba Technology Co., Ltd) was used to excite the ultrasonic wave with a 0.65 μJ YAG laser (pulse width: 2 ns, a beam diameter: 0.5 mm). In the system, the laser was input into a galvanometer mirror. The precise rotation of the mirror can control the direction of the laser beam. With the help of the system, the waveform data set

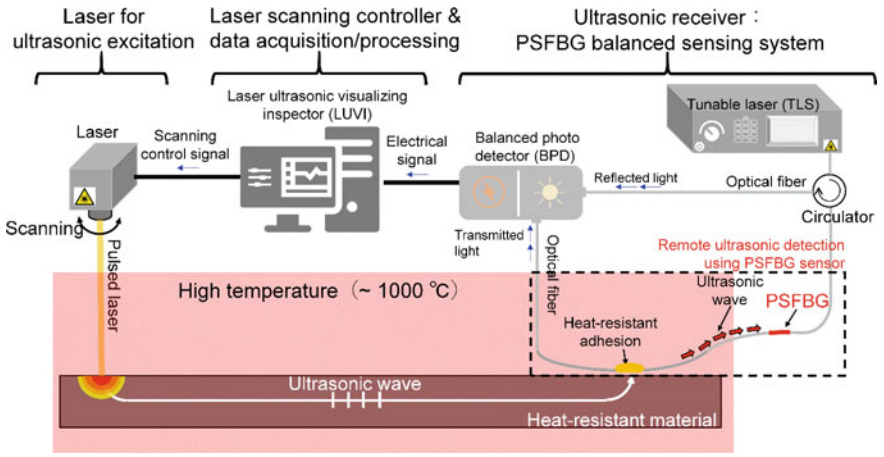

Fig. 1 Architecture of a laser ultrasonic measurement by the remotely installed PSFBG ultrasonic sensing system

used for visualizing the propagation of ultrasonic waves in a specific area can be generated by an automatic laser scan.

The remotely installed PSFBG was used as a sensor to receive ultrasonic waves during the laser scan, as illustrated on the right side of Fig. 1. In the remote ultrasonic measurement, the laser ultrasonic wave propagates from the irradiation point to the adhesion point as a guided wave in the structure. At the adhesion point, the wave transforms into a basic longitudinal wave, with an axial strain component in the core of the optical fiber, and a basic flexural wave, which primarily consists of the shear strain component in the core. Reference [8] has clarified that the PSFBG sensor selectively receives the longitudinal wave but does not receive the transverse wave because the PSFBG inscribed in the core (ϕ 10 μm) of the glass fiber (ϕ 125 μm, without polymer coating) is only sensitive to the axial strain. In addition, since the longitudinal mode exhibits no dispersion in the optical fiber, the waves propagate along the optical fiber retaining their original waveform information at the adhesion point until arriving at the sensing point. Hence, the ultrasonic waveguide formed with the optical fiber enables accurate ultrasonic measurement with the PSFBG sensor. Moreover, the ultrasonic damping in the optical fiber is so small that the remote measurement is feasible with the length of the waveguide exceeding 500 mm. In addition, since the ultrasonic waveguide formed by the silica-made optical fiber has the inherent characteristic of heat resistance, the remotely installed PSFBG sensor can perform appropriate ultrasonic measurements with excellent stability even at a temperature of 1000 °C.

In this research, the PSFBG was connected to a balanced sensing system [7] to demodulate the Bragg wavelength shift caused by the strain perturbation of the ultrasonic wave. In the system, a tunable laser (TLS, Agilent 81682A) was used as a light source to input a very narrow-band light into the PSFBG through a circulator.

Then, both the transmitted light and the reflected light from the PSFBG were guided into a balanced photodetector (BPD, New focus 2117). In the BPD, the two light components are subjected to differential processing to remove the laser intensity noise in the system and double the AC components corresponding to the dynamic strain in the PSFBG.

The optical power is then converted into an electrical signal at the BPD. After being gained via an amplifier, the waveform signals are acquired by the abovementioned LUVI system. Images of the wave propagating in the objective region are synthesized from the recorded waveform data in the system. The details of the data processing and the principle of ultrasonic visualization are explained in the next section.

2.2 Principle of Ultrasonic Visualization

Reference [10] suggested that ultrasonic waves are reversible in a measurement system of laser ultrasonics. It means that a waveform excited by laser illumination at one point and received by a sensor at another point is equivalent to the waveform that is excited at the position of the sensor and acquired around the illumination point inversely.

In this research, we assume that the reversibility is also applicable to our PSFBG sensing system. In Fig. 2 (a), ① , ② , and ③ denote three examples of laser illumination points; ***A*** and ***B*** depict the adhesion point of the optical fiber and the position of the PSFBG sensor, respectively. In real ultrasonic detection, one waveform detected by the PSFBG sensor corresponds to a one-time wave excitation at each laser illumination point. Figure 2b shows the examples of the detected burst waveforms corresponding to the three pulsed laser illumination points. A waveform group is acquired to evaluate a two-dimensional (2-D) wavefield by the automatic laser scan within the defined area. All waveform data are labeled by the positions of illumination points. Hence, the acquired data set can be treated as a three-dimensional (3-D) data matrix. Since an ultrasonic wave guided by the optical fiber is nondispersive, the 3-D data matrix acquired at point ***B*** (PSFBG sensor) is also able to accurately reflect the propagation behavior of an ultrasonic wave at point ***A*** (adhesion point).

Moreover, based on the reversibility of wave propagation, the above-collected data can inversely represent the propagation of ultrasonic waves that are excited at the fixed-point ***A*** and received at each illumination point, as illustrated in Fig. 2c. Hence, the amplitudes at a specific time of all recorded ultrasonic waves are plotted at the corresponding illumination locations in a contour map as brightness to synthesize one frame. The frame displays the magnitude distribution of the ultrasonic wave propagating from the ***A*** into the defined area at the time. Finally, the ultrasonic wave can be visualized by the continuous showing of the time-series frames. Some examples obtained in a practical demonstration of laser ultrasonic visualization with the PSFBG sensor are provided in Fig. 2d.

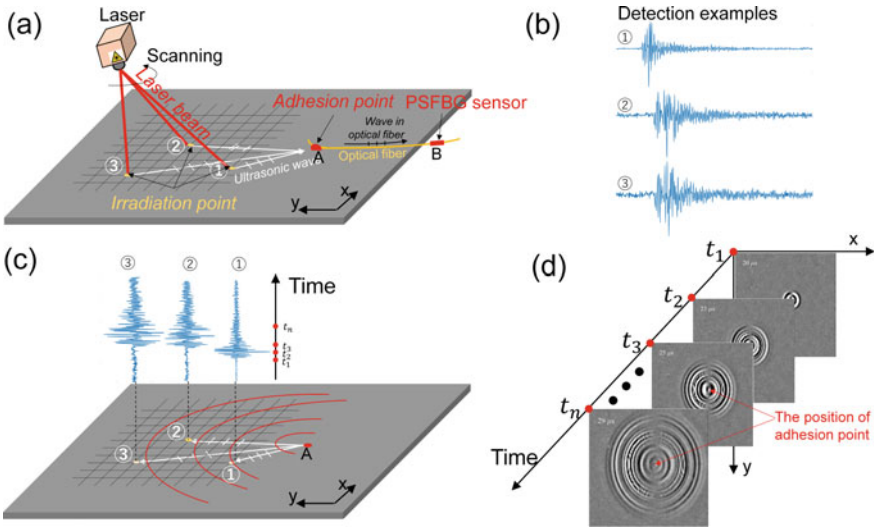

Fig. 2 Principle of laser-ultrasonic visualization technology using the remotely installed PSFBG sensor. **a** The schematic diagram of an experiment for collecting the waveform data set. **b** The examples of the detected ultrasonic signals. **c** An illustration for the process of visualizing ultrasonic waves based on the detected waveform data. **d** The examples of visualized results for the propagation of the ultrasonic wave

3 Experiments of High-Temperature Laser Ultrasonic Visualization

An experiment was conducted to verify the ability of the proposed system to visualize ultrasonic waves propagating in a SiC ceramic plate heated at a temperature of 1000 °C. Figure 3a illustrates the experimental setup. A heater capable of heating up to 1000 °C was produced by winding a Kanthal wire around a ceramic rod and then installed in an open furnace made of ceramic fiberboard. A heat-resistant glass plate transmissive for laser lights was placed over the sample as the cover of the open furnace. The laser was irradiated from the laser oscillator placed above the furnace. The laser beam penetrates through the glass plate and illuminates the surface of the specimen in the furnace for wave excitation. A scanning area of 145 mm in length and 20 mm in width was defined to match the size of the ceramic specimen. We allocated 101 grid points of laser illumination along the X-axis (the longitudinal direction) and 21 along the Y-axis (the transverse direction) in the specified area. To reduce noise in the detected ultrasonic signals, 32 waveforms were excited and averaged at each point. The optical fiber was bonded to the back surface of the ceramic plate by heat-resistant carbon paste (G7716, Ted Pella, Inc.) to transmit the laser ultrasonic waves from the ceramic plate to the PSFBG sensor placed outside of the furnace.

In order to demonstrate that the proposed method is effective for the damage diagnosis at high temperatures, a notch with a length of 4 mm was formed on the

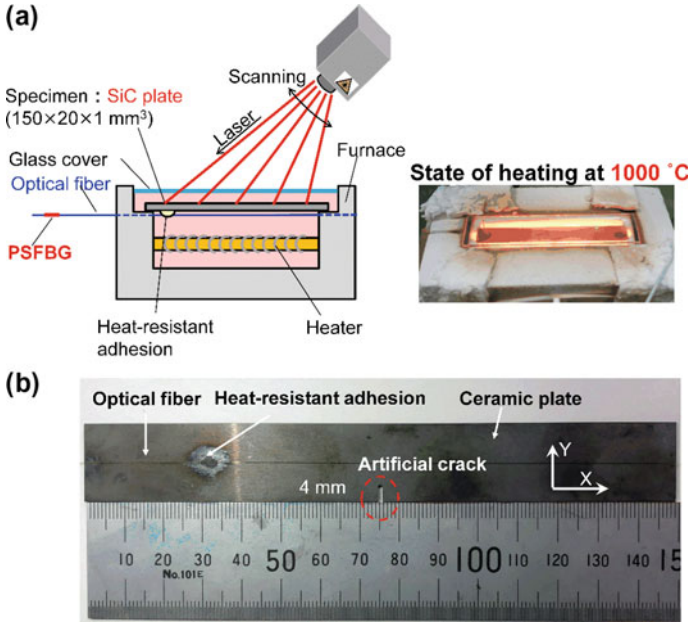

Fig. 3 Setup for the verification experiments of high-temperature laser ultrasonic visualization. **a** The configuration of the furnace and **b** The specimen with an artificial defect

lower side at a distance of 75 mm away from the left end of the plate, as shown in Fig. 3b. The width of the crack was approximately 1.5 mm, the same as the width of the cutter.

Figure 4 shows the visualization result for the ultrasonic wave propagation in the notched ceramic plate at a temperature of 1000 °C. Figure 4a represents that the wave is excited at the position of the adhesion point. The following graphs show that the wave propagates in the ceramic plate along the positive x-axis direction. This experiment verified that the laser ultrasonic measurement with the remotely installed PSFBG sensor was able to visualize the wave propagation at the temperature.

A white line denoted the position of the artificial crack in those visualization results. However, it is still difficult to identify the damage-induced change from the results because of the complicated propagation behavior of the ultrasonic wave in the SiC plate. To clarify the presence of the damage from the visualized results, we extracted the wave components corresponding to the reflection caused by an artificial defect based on a wavenumber-frequency analysis. The procedure of the analysis is described as follows.

As previously mentioned in Sect. 2.2, the visualization results for wave propagation are synthesized from a 3-D matrix of time–space data. After the 3-D Fourier transform (FT) was applied to the matrix, a spectral representation is obtained with three orthogonal variables, k_x, k_y, and f, which correspond to the ultrasonic wavenumbers along the X-axis direction and Y-axis direction and the frequency,

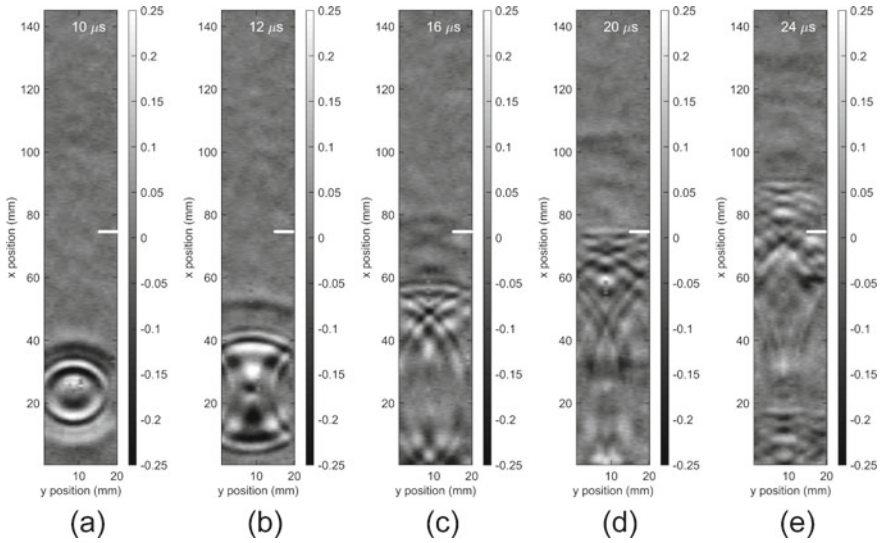

Fig. 4 Visualization of an ultrasonic wave in a specimen with an artificial defect at 1000 °C

respectively. In the wavenumber-frequency domain, the visualized ultrasonic wave is decomposed into infinite numbers of harmonic plane waves. If f is assumed to be a positive real number, then the propagation direction of the harmonic wave is determined by the signs of the wavenumbers k_x and k_y. In the FT results for the ultrasonic wave visualized in Fig. 4, the wave components propagating in the upward and downward directions had positive and negative k_x, respectively. Since the incident wave propagates in the upward direction, the crack-caused reflection wave can be extracted by filtering the wave component with negative k_x from the 3-D FT results. The direction can be further specified by determining the sign of k_y. For instance, when selecting the harmonic wave with negative k_y from the backward-direction wave, we can extract the wave components propagating in the lower-left direction in Fig. 4. Lastly, the extracted harmonic plane waves are composed together by an inverse 3D FT to restructure the filtered visualization results in the time–space domain again.

The above process was employed to separate the backward waves from Fig. 4c. In Fig. 5a, a spatial window was applied to the original image to highlight the wave components propagating from 30 to 85 mm in the longitudinal direction. Figure 5b represents the wave components propagating in the lower-left directions. A comparison between Fig. 5a and b reveals that the reflection wave is generated after the incident wave passes through the artificial defect. Moreover, a comparison among Fig. 4a, b, and c indicates that the reflection at 16 μs is caused by the fastest mode arriving at the notch earlier than the other wave modes. In accordance with the dispersive characteristics of Lamb waves in a planar structure, the firstest mode was identified as the basic symmetric (S_0) mode, which has the highest group velocity in the isotropic solid media. Figure 6 gives another example at 24 μs when the basic

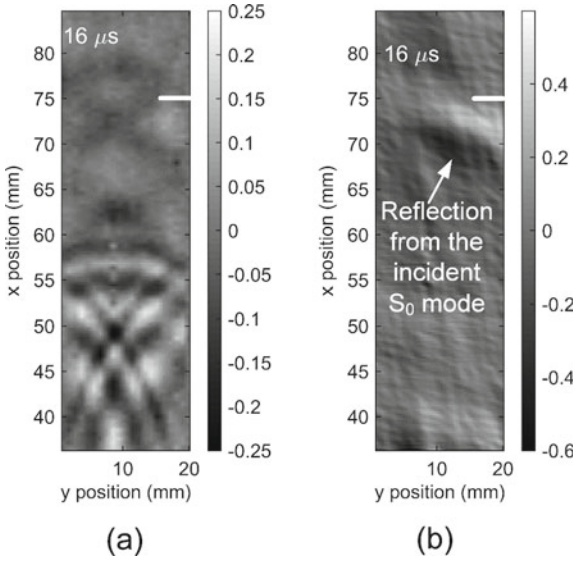

Fig. 5 Wave decomposition result based on wavenumber-frequency filtering at 16 μs. **a** The original result. **b** The lower-left backward wave

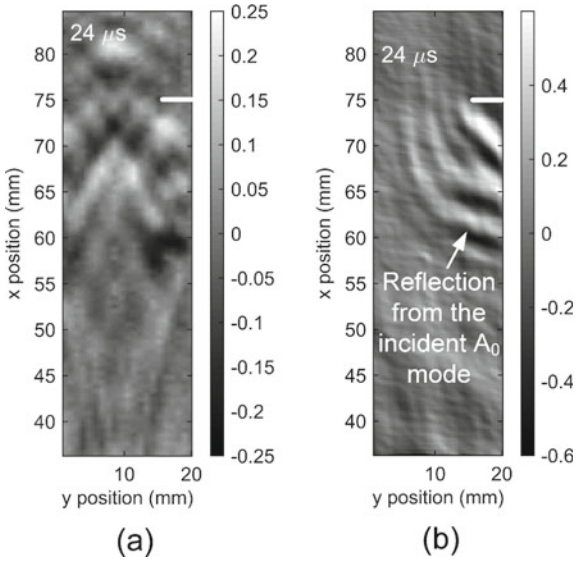

Fig. 6 Wave decomposition result based on wavenumber-frequency filtering at 24 μs. **a** The original result. **b** The lower-left backward wave

asymmetric (A_0) mode is reflected by the notch. This result indicates that the wave components corresponding to the A_0 mode have a wavelength shorter than S_0. It is also able to predict the position of the damage from the source of the backward wave of A_0.

4 Conclusions

In this research, the combination of the remote PSFBG ultrasonic sensing configuration and the LUVI system enabled a successful laser ultrasonic visualization for a heat-resistant specimen at a temperature of 1000 °C. In addition, a clear damage diagnosis was achieved by observing the image of the crack-reflected wave components filtered from the visualization result. Because of the enhanced performance, the PSFBG-based laser ultrasonic visualization system potentially contributes to establishing a comprehensive and efficient high-temperature SHM approach for heat-resistant structures.

Acknowledgements This work was supported by JST A-STEP (JPMJTR20R3) and JSPS KAKENHI Grant Number JP18H01332. This work was also supported by Japan Boiler Association Grants in Aid for Research on Boilers and Pressure Vessels.

References

1. Mitra M, Gopalakrishnan S (2016) Guided wave based structural health monitoring: a review. Smart Mater Struct 25:053001
2. Giurgiutiu V (2014) Chapter 12 - Wave propagation SHM with PWAS transducers, structural health monitoring with piezoelectric wafer active sensors, 2nd edn, pp 639–706
3. Mihailov SJ (2012) Fiber Bragg grating sensors for harsh environments. Sensors 12
4. Wu Q, Okabe Y, Yu F (2018) Ultrasonic structural health monitoring using fiber Bragg grating. Sensors 18
5. Hill KO, Meltz G (1997) Fiber Bragg grating technology fundamentals and overview. J Lightwave Technol 15:1263–1276
6. Deepa S, Das B (2020) Interrogation techniques for pi-phase-shifted fiber Bragg grating sensor: a review. Sens Actuator A-Phys 315:112215
7. Wu Q, Okabe Y (2012) High-sensitivity ultrasonic phase-shifted fiber Bragg grating balanced sensing system. Opt Express 20:28353–28362
8. Yu F, Okabe Y, Wu Q, Shigeta N (2016) Fiber-optic sensor-based remote acoustic emission measurement of composites. Smart Mater Struct 25:105033.
9. Yu F, Okabe Y (2017) Fiber-optic sensor-based remote acoustic emission measurement in a 1000 °C environment. Sensors 17
10. Takatsubo J, Yashiro S, Tsuda H, Toyama N, Lee JR, Ogisu T (2007) Nondestructive detection of delamination and debonding of CFRP by a laser-based ultrasonic visualization method. Proc SPIE Int Soc Opt Eng 6531
11. Ruzzene M (2007) Frequency–wavenumber domain filtering for improved damage visualization. Smart Mater Struct 16:2116–2129
12. Toyama N, Ye J, Kokuyama W, Yashiro S (2018) Non-contact ultrasonic inspection of impact damage in composite laminates by visualization of lamb wave propagation. Appl Sci 9
13. Lee J, Shin H, Chia CC, Dhital D, Yoon D, Huh Y (2011) Long distance laser ultrasonic propagation imaging system for damage visualization. Opt Lasers Eng 49:1361–1371
14. Park B, An Y, Sohn H (2014) Visualization of hidden delamination and debonding in composites through non-contact laser ultrasonic scanning. Compos Sci Technol 100:10–18
15. Saito O, Higuchi N, Sen E, Okabe Y (2019) Analysis of ultrasonic waves generated by oblique incidence of a laser. Insight - Non-Destr Test Cond Monit 61:714–719